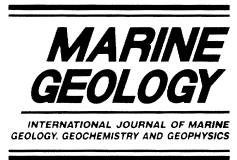




ELSEVIER

Marine Geology 153 (1999) 57–75



Holocene Climate Optimum and Last Glacial Maximum in the Mediterranean: the marine oxygen isotope record

Eelco J. Rohling*, S. De Rijk

Department of Oceanography, Southampton University, Southampton Oceanography Centre, European Way, Southampton, Hampshire SO14 3ZH, UK

Received 15 May 1997; accepted 3 February 1998

Abstract

Reconstructions with comprehensive estimates of confidence intervals are presented of changes in the W–E stable oxygen isotope gradient in Mediterranean surface waters between the Holocene Climate Optimum and the Present, and between the Last Glacial Maximum and the Present. Rigorous statistical assessment is made of the significances of the mean geographic trends observed in these reconstructions. Firstly, it is concluded that any reconstruction should strictly be based on values obtained by analyses of one single foraminiferal species throughout the basin, as different species are found to respond with isotopic variations of different amplitudes to climatic/hydrographic change. This difference is tentatively related to differences between the habitats and seasons of growth of the various species. Secondly, a significant increase of roughly a factor 3 is found in the Mediterranean W–E oxygen isotope gradient during the Last Glacial Maximum, relative to the Present. This difference is almost entirely due to increased glacial values in the Levantine Sea, which are considered to be a result of a combination of increased evaporation rates and/or somewhat cooler than anticipated surface water conditions. Thirdly, an eastward increase of roughly half the present-day magnitude is found for the W–E oxygen isotope gradient during the Holocene Climate Optimum. Values in the Levantine Sea appear to have undergone up to 0.3% more depletion than those elsewhere in the eastern Mediterranean. However, no significant trends are found between the eastern and western parts of the Levantine Sea, nor between values near the Nile delta and those from elsewhere in the Levantine Sea. The Holocene Climate Optimum's eastward increase in the Mediterranean oxygen isotope gradient, although weaker than the Present, suggests that the Mediterranean continued to function as a concentration basin, albeit in a less vigorous way than today. Finally, simple mixing arguments are used to argue that inferred oxygen isotope ratios of surface waters may not be used as an indication of conservative property (e.g. salinity) distribution on geological timescales, but instead show amplitudes of response to climatic/hydrographic changes that likely are >2 times larger than the corresponding amplitudes of response for truly conservative properties. © 1999 Elsevier Science B.V. All rights reserved.

Keywords: Last Glacial Maximum; Holocene; Mediterranean; oxygen isotopes; palaeoclimatology

* Corresponding author. Fax: +44 (1703) 593059; E-mail: e.rohling@soc.soton.ac.uk

1. Introduction

The changes in oxygen isotopic composition of planktonic foraminiferal carbonate ($\delta^{18}\text{O}_{\text{foraminiferal carbonate}}$, hereafter named δ_{fc}) from the Mediterranean have contributed strongly to speculations on the temporal variability of the Mediterranean freshwater cycle and the related thermohaline circulation (e.g. Vergnaud-Grazzini et al., 1977, 1986a,b, 1988; Jenkins and Williams, 1984; Pujol and Vergnaud-Grazzini, 1989; Thunell and Williams, 1989; Tang and Stott, 1993; Fontugne et al., 1994; Kallel et al., 1997). To derive such conclusions, δ_{fc} for any time slice in the past is compared with the present-day δ_{fc} value at the same location, measured on the same species to exclude metabolic ‘vital’ effects. Thereafter, the difference is corrected for the ‘glacial effect’, the concentration effect related to preferential uptake of ^{16}O with evaporation and subsequent storage of that relatively ^{16}O -rich water in the glacial ice sheets (e.g. Mix and Ruddiman, 1984; Labeyrie et al., 1987; Shackleton, 1987; Fairbanks, 1989, 1990).

The remainder of the $\delta_{\text{fc}}^{\text{past}} - \delta_{\text{fc}}^{\text{present}}$ difference is then viewed as a measure of two effects: (a) the ‘growth temperature effect’, which concerns the change in fractionation between seawater $\delta^{18}\text{O}$ (δ_{w}) and δ_{fc} that amounts to an enrichment by 0.2‰ per 1°C cooling, or 0.2‰ depletion per 1°C warming (cf. O’Neil et al., 1969); (b) the ‘salinity’ effect. The latter is a popular name for what would be more aptly called the ‘freshwater budget effect’. It concerns the isotopic change in the seawater (δ_{w}) through enrichment by evaporation and depletion by freshwater input (precipitation/run-off). To establish the ‘salinity effect’, sea surface temperature (SST) changes are estimated through independent methods — such as transfer functions, modern analogue functions and/or organic biomarker studies — and the $\delta_{\text{fc}}^{\text{past}} - \delta_{\text{fc}}^{\text{present}}$ difference after correction for the ‘glacial effect’ is adjusted to eliminate the effects of SST changes between the past time slice and the present. The remaining ‘isotopic residual’ is then often translated into a corresponding salinity change on the basis of a modern salinity: $\delta^{18}\text{O}$ ($S : \delta_{\text{w}}$) relationship typical for the study area (e.g. Thunell and Williams, 1989; Maslin et al., 1995; Labeyrie et al., 1996; Hemleben et al., 1996; Kallel et al., 1997).

The present paper concerns reconstruction of changes in the Mediterranean W–E δ_{w} gradient between the Holocene Climate Optimum (the time of deposition of sapropel S_1) and the Present, and between the Last Glacial Maximum and the Present. These reconstructions are interpreted in terms of climatological forcing over the Mediterranean basin. This first part of the study bears much similarity to previous syntheses of available data (Thunell and Williams, 1989; Kallel et al., 1997), but it adds new data and extensive statistical assessments of the various trends observed in the major Mediterranean sub-basins. Then follows a discussion on the potential bias introduced when reconstructing gradients using mostly *Globigerina bulloides* based isotopic records in the western Mediterranean and predominantly *Globigerinoides ruber* based records for the eastern Mediterranean. Finally, simple arguments are presented to define whether or not, and to what extent, δ_{w} behaves as a truly conservative property (such as salinity). Thus, it is evaluated whether or not the modern $S : \delta_{\text{w}}$ ratio might be applied to characterise past changes in Mediterranean salinity.

2. Data

2.1. Selection and related accuracy of data

Oxygen isotope data were obtained from various sources (see Table 1; Fig. 1 for locations), for three time slices: the Present (hereafter named 0 BP); the period between 7 and 8 ka BP (named 7/8k BP); and the Last Glacial Maximum (LGM).

Most data used to characterise the 0 BP time slice are in fact core-top data, which in piston cores may be as much as several thousands of years old (e.g. see Fontugne et al., 1989; Rohling et al., 1993). The implicit assumption is that little change occurred in the Mediterranean basin over the last two to three thousand years, which is an oversimplification that may cause several tenths of ‰ error in the 0 BP data. Box-core top results are more likely to approach the true modern conditions (e.g. Troelstra et al., 1991), although dating techniques such as ^{210}Pb would have to be routinely applied to check the age of the surface sediments.

Values for the 7/8k BP time slice were selected on the basis of time–stratigraphic frameworks pro-

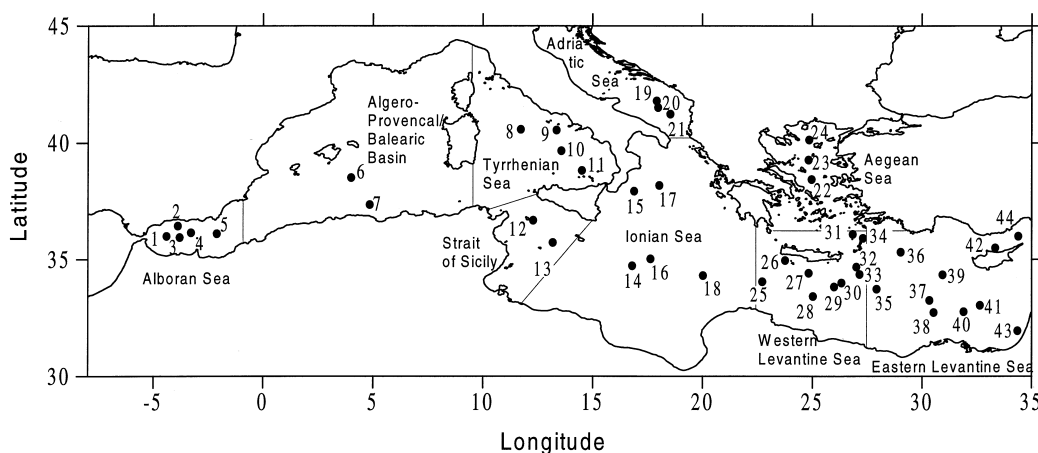


Fig. 1. Map of the Mediterranean Sea, with names of sub-basins as used in this paper and locations of the data points as listed and numbered in Table 1.

vided in the source studies. Where no depth–age calibration was provided, the most depleted value in the approximately right age range has been selected. In undated eastern Mediterranean records, the time slice was identified by the Holocene sapropel S₁, the formation period of which overlapped with the 7/8k BP time slice (e.g. Jorissen et al., 1993; Fontugne et al., 1994). Where datings were provided, the most depleted value appeared to be sometimes older and sometimes younger than 7/8k BP. As a precautionary measure, no value has been derived for the 7/8k BP time slice when the most depleted value formed a very conspicuous single outlier relative to the general isotopic profile. Still, the bias introduced by using the most depleted value from undated records is very difficult to evaluate. AMS¹⁴C dating has, however, only been performed on a routinely basis during the last decade, and using only $\delta^{18}\text{O}$ values measured during that period would severely reduce the total number of observations. The uncertainties caused by inaccurate definition of the time slice and/or the use of most depleted values, likely introduce errors of several tenths of ‰ in the 7/8k BP data. In similar ways, the LGM data listed in Table 1 are in fact the most enriched values between approximately 16 and 20k BP, unless the record had been sufficiently dated, in which case the value found nearest to 18k BP has been used.

In cores for which isotopic records were presented for several species, maximum depletions and

enrichments were not necessarily found at similar levels for the various species (e.g. core KS70-06; Vergnaud-Grazzini et al., 1986a). In such cases, values were read at that level where the maximum depletion or enrichment was found in the most representative species (usually *Globigerinoides ruber*).

2.2. Analytical precision

Modern mass spectrometers measure $\delta^{18}\text{O}$ from acidified carbonate samples with an analytical precision of order $\pm 0.1\text{‰}$ (Tang and Stott, 1993; Sikes and Keigwin, 1994). Multiple replicate analyses using single foraminifera of the same species from one and the same sample indicate standard deviations from the mean of order $\pm 0.2\text{‰}$ (Tang and Stott, 1993). Here, the ‘mean’ is the mean mass balanced value based on the various single-foram analyses, which represents the value that would be obtained should all these foraminifera be measured in one multi-foram analysis. The standard deviation of the mean from Tang and Stott (1993), therefore, provides a measure of the accuracy of multi-foram analyses ($\pm 0.2\text{‰}$) and so of the reproducibility, in addition to the $\pm 0.1\text{‰}$ limits of analytical precision. Combined, these margins define an experimental error for each multi-foram analysis of up to $\pm 0.3\text{‰}$.

Table 1
Summary of all data points used in this paper, subdivided according to location (see Fig. 1)

Basin/core	Species	Top (0k BP)	7/8k BP	LGM	7/8-0	LGM-0	LGM-7/8	Source	Lat.	Long.	Number
Alboran Sea:											
KC82-41	<i>bulloides</i>	-0.04	0.43	2.42	0.39	2.38	1.99	Pujol and Vergnaud-Grazzini, 1989	36.00°N	04.24°W	1
KS82-30	<i>bulloides</i>	-0.65	0.46	2.8	-0.19	2.15	2.34	Pujol and Vergnaud-Grazzini, 1989	36.27°N	03.53°W	2
KS82-30	<i>ruber</i>	-0.07	-0.76		-0.83			Pujol and Vergnaud-Grazzini, 1989	36.27°N	03.53°W	
SU81-07	<i>bulloides</i>	-0.81	0.66	3.7	-0.15	2.89	3.04	Kallel et al., 1997	35.57°N	03.48°W	3
KS82-31	<i>bulloides</i>	-0.24	0.62	1.86	0.38	1.62	1.24	Pujol and Vergnaud-Grazzini, 1989	36.09°N	03.17°W	4
KS82-31	<i>ruber</i>	-0.27	0.49		0.22			Pujol and Vergnaud-Grazzini, 1989	36.09°N	03.17°W	
KS82-32	<i>bulloides</i>	-0.37	0.21	3.5	-0.16	3.13	3.29	Pujol and Vergnaud-Grazzini, 1989	36.07°N	02.07°W	5
Algero-Provencal/Balearic basin:											
KS70-06	<i>ruber</i>	-0.5	-0.1	3.2	-0.6	2.7	3.3	Vergnaud-Grazzini et al., 1986a	38.31°N	04.00°E	6
KS70-06	<i>bulloides</i>	-1.5	2	3.3	0.5	1.8	1.3	Vergnaud-Grazzini et al., 1986a	38.31°N	04.00°E	
KS70-06	<i>inflata</i>	-1.6	1.7	3	0.1	1.4	1.3	Vergnaud-Grazzini et al., 1986a	38.31°N	04.00°E	
1960,201	<i>ruber</i>	-0.3	-0.6		-0.3			Buckley and Johnson, 1988	37.21°N	04.51°E	7
1960,201	<i>inflata</i>	-1.6	1.5	2.3	-0.1	0.7	0.8	Buckley and Johnson, 1988	37.21°N	04.51°E	
Tyrrhenian Sea:											
KET80-22	<i>bulloides</i>	-1.58	1.24	3.87	-0.34	2.29	2.63	Paterne et al., 1986	40.35°N	11.43°E	8
KET80-19	<i>bulloides</i>	-1.54	0.77	3.7	-0.77	2.16	2.93	Kallel et al., 1997	40.33°N	13.21°E	9
KET80-19	<i>ruber</i>	-0.71	-0.08	3.1	-0.79	2.39	3.18	Kallel et al., 1997	40.33°N	13.21°E	
KET80-04	<i>bulloides</i>	-1.67	1.23	3.94	-0.44	2.27	2.71	Paterne et al., 1986	39.40°N	13.34°E	10
KET80-03	<i>bulloides</i>	-1	0.4	3.4	-0.6	2.4	3	Kallel et al., 1997	38.49°N	14.30°E	11
KET80-03	<i>bulloides</i>	-1.43	0.79	3.83	-0.64	2.4	3.04	Paterne et al., 1986	38.49°N	14.30°E	
Strait of Sicily:											
CS72-37	<i>bulloides</i>	-1.31	0.7	3.7	-0.61	2.39	3	Kallel et al., 1997	36.41°N	12.17°E	12
CS72-37	<i>ruber</i>	-0.22	-0.54	2.8	-0.76	2.58	3.34	Kallel et al., 1997	36.41°N	12.17°E	
CS70-05	<i>bulloides</i>	-0.77	0.31	3.07	-0.46	2.3	2.76	Vergnaud-Grazzini et al., 1988	35.44°N	13.11°E	13
Ionian Sea:											
T87/26B	<i>ruber</i>	-0.25	-1		-0.75			Troelstra et al., 1991	34.44°N	16.46°E	14
KET82-22	<i>ruber</i>	-0.03	-0.78	2.55	-0.81	2.52	3.33	Fontugne et al., 1989	37.56°N	16.53°E	15
MD84-658	<i>ruber</i>	-0.58	-0.45	2.4	-1.03	1.82	2.85	Fontugne et al., 1989	35.02°N	17.38°E	16
RC9-191	<i>ruber</i>	-0.59	-0.86	3.2	-1.45	2.61	4.06	Fontugne et al., 1989; Kallel et al., 1997	38.11°N	18.02°E	17
BAN84 09GC	<i>ruber</i>	-0.7	-0.7	3	-1.4	2.3	3.7	Cheddadi et al., 1991	34.19°N	20.01°E	18
Adriatic Sea:											
IN68-9	<i>bulloides</i>	-1.6	1.3	4	-0.3	2.4	2.7	Rohling et al., 1997	41.48°N	17.55°E	19
KET82-16	<i>ruber</i>	-0.79	-0.2	3.38	-0.99	2.59	3.58	Fontugne et al., 1989	41.31°N	17.59°E	20
IN68-5	<i>bulloides</i>	-1.6	0.8		-0.8			Rohling et al., 1993	41.14°N	18.32°E	21
Aegean Sea:											
Core 20	<i>ruber</i>	-0.8	0.2		-0.6			Aksu et al., 1995	38.26°N	24.58°E	22
Core 19	<i>ruber</i>	-0.4	-0.1		-0.5			Aksu et al., 1995	39.16°N	24.50°E	23
Core 03	<i>ruber</i>	-0.4	-0.1		-0.5			Aksu et al., 1995	40.08°N	24.51°E	24

Table 1 (continued)

Basin/core	Species	Top (0k BP)	7/8k BP	LGM	7/8-0	LGM-0	LGM-7/8	Source	Lat.	Long.	Number
Levantine Sea:											
TR171-24	<i>bulloides</i>	-2.45	1.34	3.85	-1.11	1.4	2.51	R.C. Thunell and D.F. Williams, pers. commun., 1996	34.03°N	22.43°E	25
T87/2/20G	<i>ruber</i>	-1.08	-0.33	3.39	-1.41	2.31	3.72	Rohling et al., 1993	34.58°N	23.45°E	26
MO67-03	<i>ruber</i>	-1.4	-0.5	4.7	-1.9	3.3	5.2	Vergnaud-Grazzini et al., 1986a	34.25°N	24.50°E	27
RC9-181	<i>ruber</i>	-0.1	-1.2	3	-1.3	2.9	4.2	Vergnaud-Grazzini et al., 1977	33.25°N	25.01°E	28
TR171-27	<i>bulloides</i>	-1.03	0.5		-0.53			R.C. Thunell and D.F. Williams, pers. commun., 1996	33.50°N	25.59°E	29
TR171-27	<i>ruber</i>	-0.41	-1.08		-1.49			R.C. Thunell and D.F. Williams, pers. commun., 1996	33.50°N	25.59°E	
TR171-27	<i>universa</i>	-0.26	0.15		-0.11			R.C. Thunell and D.F. Williams, pers. commun., 1996	33.50°N	25.59°E	
TR171-27	<i>aequilat.</i>	-1.31	1.08		-0.23			R.C. Thunell and D.F. Williams, pers. commun., 1996	33.50°N	25.59°E	
TR171-27	<i>ruber</i>	-0.05	-1.13		-1.18			Tang and Stott, 1993	33.50°N	25.59°E	
TR171-27	<i>universa</i>	-0.87	0.46		-0.41			Tang and Stott, 1993	33.50°N	25.59°E	
TR171-27	<i>aequilat.</i>	-1.18	0.93		-0.25			Tang and Stott, 1993	33.50°N	25.59°E	
TR171-27	<i>ruber pinl.</i>	-0.63	-1.23		-0.6			Tang and Stott, 1993	33.50°N	25.59°E	
TR171-27	<i>saccul</i>	-0.05	-0.32		-0.27			Tang and Stott, 1993	33.50°N	25.59°E	
KS75-52	<i>ruber</i>	-0.1	-0.6	3.2	-0.7	3.1	3.8	Vergnaud-Grazzini et al., 1986a	34.00°N	26.19°E	30
V10-49	<i>ruber</i>	-0.58	-0.91	3.2	-1.49	2.62	4.11	Kallel et al., 1997	36.05°N	26.50°E	31
KS75-50	<i>ruber</i>	-0.2	-1.8	3.5	-1.6	3.7	5.3	Vergnaud-Grazzini et al., 1986a	34.41°N	27.00°E	32
KS82-01	<i>ruber</i>	-0.2	-0.2	3.4	-0.4	3.2	3.6	Vergnaud-Grazzini et al., 1986a	34.22°N	27.09°E	33
V10-51	<i>ruber</i>	-0.52	-1.02	3.1	-1.54	2.58	4.12	Kallel et al., 1997	35.55°N	27.18°E	34
RC9-178	<i>ruber</i>	-0.12	-1.25	3.3	-1.37	3.18	4.55	Kallel et al., 1997	33.44°N	27.55°E	35
TR171-22	<i>bulloides</i>	-1.14	0.69	3	-0.45	1.86	2.31	Thunell and Williams, 1989; R.C. Thunell and D.F. Williams, pers. commun., 1996	35.19°N	29.01°E	36
TR171-22	<i>ruber</i>	-0.54	-0.59		-1.13			R.C. Thunell and D.F. Williams, pers. commun., 1996	35.19°N	29.01°E	
TR171-22	<i>inflata</i>	-1.79	1.41		-0.38			R.C. Thunell and D.F. Williams, pers. commun., 1996	35.19°N	29.01°E	
TR171-22	<i>universa</i>	-1.3	0.49		-0.81			R.C. Thunell and D.F. Williams, pers. commun., 1996	35.19°N	29.01°E	
TR171-22	<i>aequilat.</i>	-1.28	1.08		-0.2			R.C. Thunell and D.F. Williams, pers. commun., 1996	35.19°N	29.01°E	
CHN119-16PG	<i>ruber</i>	-0.72	-0.23		-0.95			Jenkins and Williams, 1984	33.15°N	30.20°E	37
P6508-36B	<i>ruber</i>	-0.49	-0.88	2.97	-1.37	2.48	3.85	Jenkins and Williams, 1984	32.44°N	30.31°E	38
CHN119-18PG	<i>ruber</i>	-0.74	0.08	4.6	-0.66	3.86	4.52	Jenkins and Williams, 1984	34.21°N	30.56°E	39
CHN119-22PG	<i>ruber</i>	-0.93	-0.59		-1.52			Jenkins and Williams, 1984	32.46°N	31.53°E	40
MD84-641	<i>ruber</i>	-0.84	-1.37	3.2	-2.21	2.36	4.57	Fontugne and Calvert, 1992	33.02°N	32.38°E	41
Core 17	<i>ruber</i>	-0.75	-0.85		-0.1			H.A. Buckley, pers. commun., 1996; Buckley et al., 1982	35.30°N	33.20°E	42
GA32	<i>ruber</i>	-1	-2		-1			Luz, 1979; Vergnaud-Grazzini et al., 1986a	31.57°N	34.21°E	43
Core 190	<i>ruber</i>	-0.3	-0.4	2.9	-0.1	3.2	3.3	H.A. Buckley, pers. commun., 1996; Buckley et al., 1982	36.00°N	34.23°E	44

Core names are given as well as the planktic foraminiferal species analysed. Three levels were investigated per site: the core top (0 BP), the interval between 8 and 7 ka BP (7/8k BP) and the last glacial maximum (LGM), as discussed in the text. Then follow three columns giving the differences between 7/8k BP and 0 BP, LGM and 0 BP, and LGM and 7/8k BP values. This paper concentrates on the 7/8-0 and LGM-0 values. The next column gives full references to sources, followed by latitude and longitude of the core sites. The final column lists numbers assigned to each core, corresponding to those in Fig. 1.

2.3. Resultant error in the 7/8k–0 and LGM–0 differences

On the basis of the values for 0 BP, 7/8k BP and the LGM, the relative differences 7/8k–0 and LGM–0 have been determined (Table 1). Although no confidence intervals are presented with those differences, it needs to be borne in mind that the errors in the time slice values — as outlined above — propagate through further calculations according to:

$$(\sigma_C)^2 = [(\partial C/\partial A)\sigma_A]^2 + [(\partial C/\partial B)\sigma_B]^2$$

where $C = f(A, B)$ and σ_C , σ_A , and σ_B are the standard errors (Squires, 1988). The combined confidence intervals due to time slice definition problems (\pm several tenths of ‰) and experimental error margins (up to $\pm 0.3\%$) define a likely error margin of order $\pm 0.5\%$ per multi-foram analysis, or per mean mass balanced value based on replicate single-foram analyses. Two of such error margins would be involved in determining the 7/8k–0 and LGM–0 differences, which differences therefore are determined to within a conservatively estimated error margin of order $\pm 0.7\%$.

The estimated error margin is very large compared with the mean 7/8k–0 and LGM–0 differences listed in Table 1, but should not be used as an argument to stop further interpretations. Common sense evaluation of each case, with the large potential error margin in mind, seems to be a better way forward. Often, individual outliers may be thus identified, and eliminated from the data set or re-measured. Also, provided that analytical methods are standardised between laboratories and foraminifera of similar morphology and size are used (increasing the likelihood that specimens grew at similar depth and season), part of the total error might be considered to be of a systematic rather than random nature. It would therefore likely cancel out when determining differences between the various values. Similarly, routine AMS¹⁴C and ²¹⁰Pb dating to accurately constrain the time slices that are being compared would strongly reduce part of the total error, or at least provide a feeling for the extent to which the effects of time slice uncertainty are systematic rather than random.

We proceed using the calculated mean 7/8k–0 and LGM–0 values (Table 1) to interpret environmental changes in the Mediterranean basin. This approach (after Thunell and Williams, 1989; Kallel et al., 1997) optimistically assumes that the above outlined errors due to time slice uncertainty and experimental error are entirely systematic, and so may be ignored.

3. Statistical investigations

First, Kolmogorov–Smirnov tests were performed on the entire data set and on individual sub-sets, using the Lilliefors procedure with sample data standardisation to account for unknown mean and variance of the parent distribution (Davis, 1986, p. 99). Thus the Kolmogorov–Smirnov test may be used to compare cumulative sample distributions with a standard normal distribution function with mean = 0 and variance = 1. All cumulative distribution functions for the data were found to be significantly similar to a standard normal distribution at the level of $\alpha = 0.05$.

Next, a series of statistical tests were undertaken to compare individual sub-sets of data with one another (Table 2; Fig. 1 for areas), both for LGM–0 and for 7/8k–0 data sets. These tests investigate: (1) equality of variance, to compare the ‘quality’ of the data in one sub-set with that of the other, using a simple *F*-test with $\alpha = 0.05$ (Davis, 1986, p. 68); (2) equality of means, to evaluate whether the means of the two compared sub-sets of data are statistically similar (null hypothesis), or different (alternative hypothesis), at the level of $\alpha = 0.05$. The equality of means testing was performed for each case using three different two-tailed tests: (a) the one-way analysis of variance (ANOVA; Davis, 1986, p. 74); (b) the Student-*t* test (Davis, 1986, p. 65); and (c) the Mann–Whitney test, as a non-parametric equivalent of the Student-*t* test (Davis, 1986, p. 93). Although the Kolmogorov–Smirnov tests demonstrated normality for the parent distributions, indicating that non-parametric testing is not essential, it is still included for validation of the parametric test results.

Table 2
Listing of the statistical test results, as discussed in the text

Test A vs. B	Charact. A	Charact. B	Equality of variance $\alpha = 0.05$	One-way ANOVA $m_A = m_B$ ($\alpha = 0.05$)	Student <i>t</i> -test $m_A = m_B$ ($\alpha = 0.05$)	Non-parametric Mann–Whitney $m_A = m_B$ ($\alpha = 0.05$)	Conclusion
LGM–0:							
wM vs. eM <i>bulloides</i>	$N = 11$ $m = 2.32$ $\sigma = 0.41$ $\sigma_m = 0.12$	$N = 5$ $m = 2.07$ $\sigma = 0.39$ $\sigma_m = 0.17$	Y	Y	Y	Y	Similar
wM vs. eM <i>rub. + bull.</i>	$N = 13$ $m = 2.35$ $\sigma = 0.39$ $\sigma_m = 0.11$	$N = 24$ $m = 2.65$ $\sigma = 0.57$ $\sigma_m = 0.12$	Y	Y	Y	Y	Similar
Lev. vs. other-eM <i>ruber</i>	$N = 13$ $m = 2.99$ $\sigma = 0.48$ $\sigma_m = 0.13$	$N = 6$ $m = 2.40$ $\sigma = 0.28$ $\sigma_m = 0.12$	Y	N	N	N	Different
7/8k–0:							
wM vs. eM <i>bulloides</i>	$N = 11$ $m = -0.18$ $\sigma = 0.42$ $\sigma - m = 0.13$	$N = 6$ $m = -0.62$ $\sigma = 0.27$ $\sigma_m = 0.11$	Y	N weak	N weak	N weak	Different
wM vs. eM <i>ruber</i>	$N = 5$ $m = -0.46$ $\sigma = 0.39$ $\sigma_m = 0.17$	$N = 30$ $m = -1.07$ $\sigma = 0.50$ $\sigma_m = 0.09$	Y	N	N	N	Different
wM vs. eM <i>rub. + bull.</i>	$N = 16$ $m = -0.27$ $\sigma = 0.43$ $\sigma_m = 0.11$	$N = 36$ $m = -1.00$ $\sigma = 0.50$ $\sigma_m = 0.08$	Y	N very strong	N very strong	N very strong	Very different
wM vs. other-eM <i>ruber</i>	$N = 5$ $m = -0.46$ $\sigma = 0.39$ $\sigma_m = 0.17$	$N = 10$ $m = -0.88$ $\sigma = 0.32$ $\sigma_m = 0.10$	Y	Y	N	Y weak	Possibly different
wM vs. other-eM <i>rub. + bull.</i>	$N = 16$ $m = -0.27$ $\sigma = 0.43$ $\sigma_m = 0.11$	$N = 14$ $m = -0.78$ $\sigma = 0.33$ $\sigma_m = 0.09$	Y	N very strong	N very strong	N very strong	Very different
Lev. vs. other-eM <i>ruber</i>	$N = 20$ $m = -1.17$ $\sigma = 0.54$ $\sigma_m = 0.12$	$N = 10$ $m = -0.88$ $\sigma = 0.32$ $\sigma_m = 0.10$	Y	Y	Y	Y	Similar
Lev. vs. other-eM <i>ruber</i> excl. NNE Cyprus data	$N = 18$ $m = -1.29$ $\sigma = 0.43$ $\sigma_m = 0.10$	$N = 10$ $m = -0.88$ $\sigma = 0.32$ $\sigma_m = 0.10$	Y	N	N	N	Different
Lev. west vs. Lev. east <i>ruber</i> (separation at 27°30'E)	$N = 10$ $m = -1.30$ $\sigma = 0.42$ $\sigma_m = 0.13$	$N = 10$ $m = -1.04$ $\sigma = 0.61$ $\sigma_m = 0.19$	Y	Y	Y	Y	Similar

Table 2 (continued)

Test A vs. B	Charact. A	Charact. B	Equality of variance $\alpha = 0.05$	One-way ANOVA $m_A = m_B$ ($\alpha = 0.05$)	Student <i>t</i> -test $m_A = m_B$ ($\alpha = 0.05$)	Non-parametric Mann–Whitney $m_A = m_B$ ($\alpha = 0.05$)	Conclusion
Lev. west vs. Lev. east <i>ruber</i> (separation at 27°30'E) excl. NNE Cyprus data	$N = 10$ $m = -1.30$ $\sigma = 0.42$ $\sigma_m = 0.13$	$N = 8$ $m = -1.28$ $\sigma = 0.44$ $\sigma_m = 0.16$	Y	Y	Y	Y	Similar
Nile area vs. Lev. <i>ruber</i>	$N = 5$ $m = -1.41$ $\sigma = 0.46$ $\sigma_m = 0.20$	$N = 15$ $m = -1.09$ $\sigma = 0.54$ $\sigma_m = 0.14$	Y	Y	Y	Y	Similar

N = number of observations; m = mean; σ = sample standard deviation; σ_m = standard error of the mean (σ/\sqrt{N}). Results are organised per time slice study (LGM–0 and 7/8k–0), and the Y (Yes) and N (No) markers indicate whether or not the null hypotheses of equality of variance (column 4) and means ($m_A = m_B$; columns 5, 6, 7) are valid at the $\alpha = 0.05$ significance level. The final column summarises the outcome of the equality of means testing, in terms of similarity or dissimilarity of the tested data sets.

4. Results

4.1. Last Glacial Maximum

Statistical test results (Table 2) for the comparisons between the various sub-sets of data for the Last Glacial Maximum (LGM) to 0 BP δ_{fc} differences (LGM–0) suggest that no significant differences exist at the level of $\alpha = 0.05$ between the mean changes in δ_{fc} in the western and eastern basins; neither where only measurements on *Globigerina bulloides* are considered, nor where the combined set of measurements on *G. bulloides* and *Globigerinoides ruber* is used. Within the eastern Mediterranean data set, however, a significant ($\alpha = 0.05$) difference of about 0.50‰ is found between the means of data from the Levantine Sea and from elsewhere in the eastern Mediterranean.

4.2. Holocene climatic optimum (7/8 k BP)

The differences between the values of the period of 7/8k and 0 BP (7/8k–0; Table 1) show a more complex pattern than the LGM–0 results (Tables 1 and 2). Significant differences ($\alpha = 0.05$) are found between the mean 7/8k–0 changes of δ_{fc} in the western and eastern basins, both when considering measurements based on *G. bulloides* ($\delta_{fc}^{bulloides}$) and *G. ruber* (δ_{fc}^{ruber}) separately and combined. The mean

7/8k–0 change in δ_{fc} of the western basin is found to be significantly different from that for eastern basin values excluding Levantine data when considering the combined $\delta_{fc}^{bulloides}$ and δ_{fc}^{ruber} measurements. However, this difference is less convincing when considering only *G. ruber* based measurements. At first sight, the mean 7/8k–0 change in δ_{fc} from Levantine data shows no significant difference with that from data of the rest of the eastern Mediterranean, but this is strongly due to two low outliers of -0.1% observed north and northeast of Cyprus. Exclusion of these two points from the Levantine data set shows a generally significant ($\alpha = 0.05$) difference of 0.4‰ between the mean Levantine value and the mean value for the rest of the eastern Mediterranean. Using only δ_{fc}^{ruber} results, a significant trend appears of mean δ_{fc} changes from -0.5 , via -0.9 to -1.2% , from the western Mediterranean, via the eastern Mediterranean outside the Levantine Sea, to the Levantine Sea, respectively.

Three additional tests investigate the statistical significance of geographic trends in the depletion within the Levantine basin (Table 2; Fig. 1). These tests show no significant ($\alpha = 0.05$) differences between the means and variances for the western and eastern Levantine Sea (Fig. 1), nor between the means and variances based on records from the immediate vicinity of the Nile delta (cores 37, 38, 40, 41, 43; Table 1; Fig. 1) and those from elsewhere

in the Levantine basin. These results suggest that the maximum depletion found in the Levantine basin is more or less homogeneously distributed, rather than centred around, for instance, the Nile delta.

5. Discussion

5.1. Multi-species comparisons

From the population statistics and statistical equality tests (Table 2), it appears that δ_{fc}^{ruber} on average shows greater amplitude in its response to climatic/hydrographic changes than $\delta_{fc}^{bulloides}$, regarding both enrichments and depletions. This bias likely originates in different habitat characteristics, with *G. ruber* being a shallow mixed-layer dweller that is especially prolific in late summer and fall, while *G. bulloides* occupies a greater depth range and thrives especially in late winter and early spring (Pujol and Vergnaud-Grazzini, 1995). In the thin mixed layer above the seasonal thermocline, freshwater balance variations and heating have more pronounced effects on both δ_w and $\delta_w - \delta_{fc}$ fractionation, than in the thicker and better homogenised late winter/early spring surface waters, which may account for the larger amplitude variations found in δ_{fc}^{ruber} relative to $\delta_{fc}^{bulloides}$.

The observed amplitude differences illustrate that it is important to only compare mean δ_{fc} variations based on measurements of one single species. Bias in multi-species comparisons is exemplified by particularly strong statistical differences found for the 7/8k–0 means comparisons between the western and eastern Mediterranean entirely, and between the western Mediterranean and the eastern basin excluding Levantine data, when performed on combined *G. ruber* and *G. bulloides* data sets (Table 2). These results are artificially enhanced because of: (a) the unequal distribution of measurements, with the bulk of western Mediterranean values based on *G. bulloides* and the bulk of eastern Mediterranean values based on *G. ruber*; and (b) lower-amplitude variations in $\delta_{fc}^{bulloides}$ relative to δ_{fc}^{ruber} . These factors combined emphasise the stronger depletion in the eastern basin, and the tests show a resultant increase in the significance of the difference between the means of the western and eastern depletions.

Summarising, it appears from the statistical analy-

ses presented here that, where possible, comparisons between mean δ_{fc} variations in various locations should be based on one single species being analysed. Simple ‘corrections’ of values measured for one species to ‘virtual values’ for another by means of a constant offset are not a sensible way forward, as illustrated by the wide variability observed in δ_{fc} variations for various species from within the same sample (Table 3). This paper thus calls for increased efforts in obtaining detailed isotopic records of: (1) *G. ruber* in the western Mediterranean; and/or (2) *G. bulloides* in the eastern Mediterranean; and/or (3) other species common in both basins (e.g. right-coiling *Neogloboquadrina pachyderma*, although this species is unfortunately absent from most eastern Mediterranean Holocene intervals).

5.2. Last Glacial Maximum

5.2.1. Reconstruction of the W–E δ_w gradient

The statistical analyses of the LGM–0 data indicate that δ_{fc} was enriched more or less uniformly by about $2.50 \pm 0.15\text{‰}$ throughout the Mediterranean — from immediately east of Gibraltar to far into the eastern basin — but reached $3.0 \pm 0.13\text{‰}$ in the Levantine Sea (Table 2). Today, Mediterranean δ_w values range from 0.9 (Pierre, 1999) to $1.3 \pm 0.03\text{‰}$ in the western Mediterranean, via $1.5 \pm 0.04\text{‰}$ in the eastern central Mediterranean, to $1.7 \pm 0.04\text{‰}$ in the Levantine Sea (Pierre et al., 1986; Table 4; Fig. 2). We combine these values with the observed glacial enrichments, to determine the glacial W–E isotope trend through the Mediterranean (Table 5).

Corrections have been applied for the glacial ice volume effect, by $0.012 \pm 0.001\text{‰ m}^{-1}$, or $1.44 \pm 0.12\text{‰}$ for the LGM (cf. Labeyrie et al., 1987; Shackleton, 1987; Fairbanks, 1989), and for the influence of a different glacial surface water temperature distribution on δ_w to δ_{fc} fractionation (δ_{fc} changes by $+0.2\text{‰}$ per 1°C cooling, or -0.2‰ per 1°C warming relative to δ_w). The overview by Bigg (1995) of temperature reconstructions for the glacial Mediterranean indicates that temperature was on average about 5°C lower than today in winter throughout the basin, but also that the summer temperatures were 7° to 9°C lower than today in the western basin, 2° to 6°C lower in most of the eastern Mediterranean outside the Levantine basin, and only 1° to 2°C lower

Table 3

Overview of oxygen isotopic differences for various species within the same time slice comparisons, which illustrates the distinct differences in amplitude of isotopic change between the individual species

Core:	KS82-30	KS82-31	KS70-06	1960.201	KET80-19	CS72-37	TR171-27	TR171-27	TR171-22	KS70-06	KET80-19	CS72-37
Time slice comparison:	7/8–0 BP	LGM–0 BP	LGM–0 BP	LGM–0 BP								
Species												
<i>ruber</i>	–0.83	0.22	–0.6	–0.3	–0.79	–0.76	–1.49	–1.18	–1.13	2.7	2.39	2.58
<i>bulloides</i>	–0.19	0.38	0.5		–0.77	–0.61	–0.53		–0.45	1.8	2.16	2.39
<i>inflata</i>			0.1	–0.1					–0.38	1.4		
<i>universa</i>							–0.11	–0.41	–0.81			
<i>aequilateralis</i>							–0.23	–0.25	–0.2			
<i>ruber (pink)</i>								–0.6				
<i>sacculifer</i>								–0.27				

Full references to the sources of the values may be found in Table 1.

Table 4

Summary of water-based oxygen isotope data for surface waters in the three main sub-areas within the Mediterranean (relative to SMOW standard; after Pierre et al., 1986)

Location	Depth range (m)	N	Mean δ_w (‰ SMOW)	σ	σ_m
wMed; ST4	0–50	4	1.30	0.07	0.03
wMed; ST4	0–100	6	1.32	0.07	0.03
eMed; ST10 and 11	0–50	9	1.50	0.12	0.04
eMed; ST10 and 11	0–100	12	1.51	0.11	0.03
Lev.; ST14 and 16	0–50	8	1.70	0.10	0.04
Lev.; ST14 and 16	0–100	13	1.71	0.09	0.03

Data are separated in 0–50 averages and 0–100 m averages, with sample standard deviations and standard errors of the means.

Table 5

Summary of the procedures followed in the reconstructions of the LGM and 7/8k BP W–E δ_w gradients through the Mediterranean

	West	Central	East	
Today:				
δ_w	0.9 ^b or 1.3 ^a ± 0.03	1.5	1.7 ± 0.04	A
7/8k BP*:				
$\Delta\delta_{fc}$	–0.5 ± 0.17	–0.9	–1.2 ± 0.1	B
A + B	0.4 ^b or 0.8 ^a ± 0.2	0.6 ± 0.1	0.5 ± 0.1	C
Δ SST effect	–0.4 ± 0.1	0	0	D
C + D	0.0 ^b or 0.4 ^a ± 0.2	0.6	0.5 ± 0.1	
LGM**:				
$\Delta\delta_{fc}$	2.5 ± 0.15	2.5	3.0 ± 0.13	E
Ice vol. effect	1.44 ± 0.12	1.44	1.44 ± 0.12	F
A + E – F	2.0 ^b or 2.4 ^a ± 0.2	2.6	3.3 ± 0.2	G
Δ SST effect	1.2 ± 0.4	1.0 ± 0.4	0.6 ± 0.4	H
G – H	0.8 ^b or 1.2 ^a ± 0.5	1.6	2.7 ± 0.5	

West corresponds to western Mediterranean, Central to eastern Mediterranean excluding the Levantine Sea, and East to Levantine Sea in Tables 1 and 2.

*7/8 BP W–E gradient 0.1 to 0.2 for modern gradient of 0.4^a, or 0.5 to 0.6 for modern gradient of 0.8^b = reduced to 0.5 ± 0.25 times the present.

**LGM W–E gradient 1.5 for modern gradient of 0.4^a, or 1.9 for modern gradient of 0.8^b = increased to 3.1 ± 0.7 times the present.

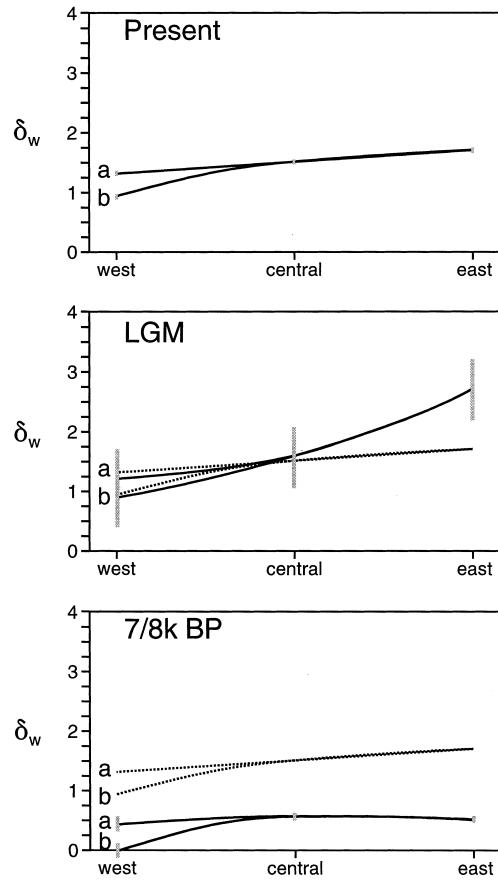


Fig. 2. Schematic presentation of the present-day W–E δ_w gradient through the Mediterranean and comparisons with that reconstructed for the period of 7/8k BP and the LGM (see Table 5). Lines marked *a* are based on the present-day observations of Pierre et al. (1986) and lines marked *b* are based on those of Pierre (1998). Line *b* may be more accurate as it accounts for modern observations from the westernmost Alboran Sea which were lacking in the earlier data set (line *a*). However, we present both lines instead of only the most recent result, to avoid potential complications from possible changes in the modern values during the last decade related to ongoing hydrographic change in the Mediterranean (e.g. Rohling and Bryden, 1992; Béthoux and Gentili, 1996).

in the Levantine Sea. Our reconstruction of the LGM W–E δ_w gradient (Table 5; Fig. 2) uses coarse average temperature corrections of $-6 \pm 2^\circ\text{C}$ for the western basin, $-5 \pm 2^\circ\text{C}$ for the eastern basin outside the Levantine Sea, and $-3 \pm 2^\circ\text{C}$ for the Levantine Sea.

We find (Table 5; Fig. 2) a robust mean glacial W–E gradient that is about 1.1‰ steeper than the

present-day gradient, with $1\sigma = (0.5^2 + 0.5^2)^{1/2} = \pm 0.7\text{‰}$. Both the LGM and the present-day gradients show eastward increase, even if the magnitudes are very different. The basin apparently acted as a concentration basin during the LGM, as it does today, but there appear to have been strong relative differences in evaporation rates.

5.2.2. Quantitative interpretation

First, the influence of 120 m glacial sea level lowering (Fairbanks, 1989, 1990; Blanchon and Shaw, 1995) on Atlantic inflow through the Strait of Gibraltar needs to be assessed. Using the Bryden and Kinder (1991) hydraulic control model with variable sea level it was found that glacial inflow volume was only about 50% of the present, assuming that the net water deficit for the Mediterranean was similar to the present (Rohling and Bryden, 1994). This alters the balance between advection and net freshwater loss, and so intensifies concentration processes in the basin.

Today, the ratio between volume of Atlantic inflow (A) and the net freshwater loss (excess of evaporation over freshwater input; X) in the Mediterranean is about 23:1.3 (Bryden et al., 1994). Conservation of mass and salt defines the relationship $X/M = \Delta S/S_A$, where M is the Mediterranean outflow into the Atlantic ($M = A - X$), ΔS the Mediterranean–Atlantic salinity difference, and S_A the salinity of Atlantic inflow into the Mediterranean. This relationship gives a present-day average increase of about 6% for salinity relative to its value in Atlantic inflow. The 50% reduction in inflow due to sea level lowering — with X equal to the present — would change the $A:X$ ratio to 11.5:1.3 at glacial times, which would result in a glacial salinity increase of 13% relative to that of Atlantic inflow. These relative increases in salinity would be typical for any conservative property that behaves similar to salinity. Consequently, glacial W–E gradients of such conservative properties would have been of approximately double magnitude compared with the present. This is not enough to explain the difference between the present-day and glacial W–E δ_w gradients, which roughly amounts to a factor 3 (Table 5; Fig. 2).

The difference between the glacial and present-day W–E δ_w gradients is predominantly due to a 1‰

higher glacial mean δ_w value in the Levantine Sea. Enhanced concentration effects related to sea level lowering would have roughly doubled the present-day gradient, giving $2 \times 0.4 = 0.8\text{‰}$ (using gradient of Pierre et al., 1986) or $2 \times 0.8 = 1.6\text{‰}$ (using gradient of Pierre, 1999). Hence, an excess 1.5– $2 \times 0.4 = 0.7\text{‰}$ or $1.9 - 2 \times 0.8 = 0.3\text{‰}$ remains to be accounted for, respectively (Table 5; Fig. 2). Excess enrichment in the glacial Levantine basin cannot be addressed in terms of relatively lower glacial influence of Nile discharge, as the modern discharge has been negligible since completion of the Aswan dam (Nof, 1979) and so has no influence on the modern δ_w gradients of Pierre et al. (1986) or Pierre (1999).

Incorrect glacial temperature distributions used in calibrating δ_{fc} to δ_w for the Levantine basin could explain part of the excess enrichment; an error of 1.5° or 3.5°C would fully account for it. Alternatively, evaporation rates from the Levantine Sea may have been higher than today. Latent heat flux in W m^{-2} , with $1 \text{ W} \equiv 1.26 \text{ cm yr}^{-1}$ per unit area, is given according to the relationship:

$$Q_L = \rho_a L C V [q_{s(T_s)} - q_a] \times 10^6$$

where ρ_a is density of air (1.2 kg m^{-3}), L is latent heat of vaporisation (weakly temperature dependent, $\sim 2.45 \text{ J kg}^{-1}$), C is the exchange coefficient (1.15×10^{-3} ; Garrett et al., 1993; Wells, 1995), V is wind speed which today averages about 7.5 m s^{-1} (based on a 45 year time series; Garrett et al., 1993), $q_{s(T_s)}$ is the saturation mixing ratio at the sea surface temperature (T_s), and $q_a = r q_{s(T_a)}$, with r being the relative humidity and $q_{s(T_a)}$ the saturation mixing ratio at the temperature T_a measured at 10 m above the sea surface (i.e. $T_s - T_a$ is the sea–air temperature difference) (Wells and King-Hele, 1990). Values for L , $q_{s(T_s)}$, and $q_{s(T_a)}$ may be read from tables, e.g. Beer (1990). Between 1945 and 1990, Mediterranean values for $q_{s(T_s)} - q_a$ ranged between 3.3×10^{-3} and 4.1×10^{-3} (Garrett et al., 1993).

The latent heat loss equation shows that significant increases in the Levantine evaporation rates could particularly have resulted from: (1) flow of colder than present glacial air masses over relatively warm Levantine waters, increasing the sea–air temperature difference; and/or (2) increased glacial mean wind speeds over the basin; and/or (3) de-

creased relative humidity in the air masses that flowed over the glacial Levantine Sea. The latter may be less likely in view of the arguments of Rozanski (1985) against substantial relative humidity changes, based on deuterium excess results. Since increased latent heat loss through evaporation would also tend to lower sea surface temperature, it seems likely that the 0.3 to 0.7‰ excess δ_w enrichment in the glacial Levantine basin resulted from a combination of increased evaporation rates and somewhat cooler than anticipated surface waters.

5.3. 7/8k BP

5.3.1. Reconstruction of the W–E δ_w gradient

Results for the 7/8k–0 δ_{fc} changes based on *G. ruber* — the only species for which a sufficient number of records is available from all parts of the Mediterranean — suggest that western Mediterranean δ_{fc} values were depleted by some $0.5 \pm 0.17\text{‰}$, increasing to depletions of about $0.9 \pm 0.10\text{‰}$ in the eastern Mediterranean outside the Levantine basin, and $1.2 \pm 0.12\text{‰}$ in the Levantine basin. Table 5 combines these values with recent (Pierre, 1998) and previous (Pierre et al., 1986) observations of the present-day W–E δ_w gradient in the Mediterranean. The late summer season of the Pierre et al. (1986) observations (Table 4) corresponds closely to the growth season of *G. ruber* in the Mediterranean, while the 0–100 m depth range of those observations encompasses its living depth (Vergnaud-Grazzini et al., 1986b; Pujol and Vergnaud-Grazzini, 1995).

There is a correction for surface water temperature differences between 7/8k BP and the present, according to recent suggestions that the 7/8k BP temperature distribution in the eastern Mediterranean was similar to the present, but that the western basin experienced 1.5° to 2.5°C lower temperatures (Kallel et al., 1997). Those values are based on modern analogue functions using planktonic foraminiferal distribution patterns, and need validation from independent methods, such as properly calibrated long-chain alkenone ratios. Using the Kallel et al. (1997) 1.5° to 2.5°C cooling values for the western basin, therefore, we possibly introduce some error, but as yet this cannot be quantified in detail.

The calculated 7/8k BP δ_w values show an eastward increase between 0.15 and $0.55 \pm 0.25\text{‰}$, rel-

ative to a present-day gradient of 0.4 (Pierre et al., 1986) or 0.8‰ (Pierre, 1998), respectively (Table 5; Fig. 2). Although the confidence intervals involved are similar in width to the signal amplitude, it is still interesting to speculate on the causes of change in the mean trend, for which purpose it is assumed that the confidence interval is at least in part of a systematic nature, and could thus be (partly) ignored. The confidence interval, however, does imply that any conclusions based on the mean trend should be treated as order of magnitude estimates of change only. A mean 7–8k BP west to east δ_w gradient is found at roughly 50% of its present-day magnitude, but of the same sign (eastward increase). This suggests that the Mediterranean continued to function as a concentration basin, albeit with a net freshwater deficit that was substantially smaller than today.

5.3.2. Quantitative interpretation

To interpret a reduction in the δ_w gradient to roughly 50% of its present-day value, it should be taken into account that reduction of net evaporation causes a decrease in inflow into the basin from the Atlantic, with both decreases being of different proportions. This alters the balance between advection and freshwater loss. The increase of conservative properties like salinity in the Mediterranean with a strait configuration similar to today, varies in accordance with the net freshwater loss (excess evaporation) to the two-thirds power: $\Delta S = X^{2/3}$ (cf. Bryden and Kinder, 1991). Assuming that δ_w behaves as a conservative property, which assumption is evaluated in the next section, a 50% reduction in $\Delta\delta_w$ would imply a decrease of X to about 35% of its present-day value.

Today, the overall water deficit for the Mediterranean Sea amounts to 52 cm yr^{-1} (Bryden et al., 1994), or $1.3 \times 10^{12} \text{ m}^3 \text{ yr}^{-1}$. The above interpretation of the roughly 50% reduced west–east δ_w gradient would, therefore, suggest that this deficit was of order $0.5 \times 10^{12} \text{ m}^3 \text{ yr}^{-1}$ in the period 7/8k BP. The inferred $0.8 \times 10^{12} \text{ m}^3 \text{ yr}^{-1}$ reduction provides interesting comparison with estimates of increased outflow of freshwater from the Black Sea following postglacial connection to the Mediterranean (Lane-Serff et al., 1997), and of a discharge maximum of the Nile River caused by intensified summer monsoons (Rossignol-Strick et al., 1982; Béthoux, 1984).

Before damming commenced in 1947, the Black Sea discharged its net freshwater gain of order $0.2 \times 10^{12} \text{ m}^3 \text{ yr}^{-1}$ into the Mediterranean, which over the next four decades decreased to about 60% of that value (Tolmazin, 1985). Lane-Serff et al. (1997) presented hydraulic arguments for the history of Black Sea outflow in the past 10,000 years, and in their most realistic scenario found that the net freshwater outflow in the period of 7/8k BP was roughly twice as large as today, i.e. increased by another $0.2 \times 10^{12} \text{ m}^3 \text{ yr}^{-1}$. Before completion of the Aswan dam, Nile discharge was of order $0.06 \times 10^{12} \text{ m}^3 \text{ yr}^{-1}$ (Béthoux and Gentili, 1996) to $0.08 \times 10^{12} \text{ m}^3 \text{ yr}^{-1}$ (Wahby and Bishara, 1981). This decreased to a negligible amount when the dam was in place (Nof, 1979), so that the Nile is of no significance to the modern δ_w gradient. Using a roughly 2.5-fold increase in Nile River flow (relative to pre-Aswan values) for the period of 7/8k BP (cf. Béthoux, 1984), the Nile discharge was of order $0.2 \times 10^{12} \text{ m}^3 \text{ yr}^{-1}$. Consequently, the combined increases of Black Sea outflow and Nile River discharge relative to the present would have made up some $0.4 \times 10^{12} \text{ m}^3 \text{ yr}^{-1}$, more or less half of the estimated total reduction in the Mediterranean water deficit.

The remaining half of the reduction would have been due to increased discharge rates of rivers other than the Nile (e.g. Shaw and Evans, 1984; Rossignol-Strick, 1987; Rohling and Hilgen, 1991; Zachariasse et al., 1997) and reduced evaporation. The latter would especially be expected for the western Mediterranean if indeed its surface temperatures were 1.5° to 2.5°C lower than today, since this would cause a reduction of order 10% in the evaporation rate (latent heat flux after Wells and King-Hele (1990) and Beer (1990); sea–air temperature difference assumed constant at 1°C).

The about $1.2 - 0.9 = 0.3\text{‰}$ stronger depletion in Levantine $\delta_{\text{fc}}^{\text{ruber}}$ values, relative to that in the rest of the eastern Mediterranean, may be interpreted as an expression of strong influence of Nile discharge in the shallow, late summer, mixed-layer in which *G. ruber* thrives. This interpretation would support the hypothesis of summer monsoon driven maxima of the Nile discharge around 7/8k BP (Rossignol-Strick et al., 1982), although the maximum depletion in the Levantine basin does not appear to be significantly centred around the Nile delta, nor in the eastern part

of the Levantine basin (Table 2). The excess depletion in the Levantine basin may also be interpreted: (1) as a result of a possibly more depleted nature of the Nile discharge at times of sapropel formation, as suggested by strongly depleted values in NW African palaeo-waters (overview in Rozanski, 1985) and in lacustrine carbonates (McKenzie, 1993); and/or (2) in terms of a possible error of about 1.5°C in the assumption that the temperature distribution over the eastern Mediterranean was similar to the present; and/or (3) in terms of a slightly decreased rate of evaporation over the Levantine basin, which might have resulted from a combination of lower mean wind speed, higher relative air humidity, and reduced air–sea temperature differences.

5.4. On the accuracy of δ_w as a proxy for salinity

In contemporary oceanography, δ_w is often used as a conservative property, representative of a water mass, and changes in δ_w are then used to detect degrees of mixing between water masses (e.g. Weiss et al., 1979; Fairbanks, 1982; Kipphut, 1990; Frew et al., 1995). Such use of δ_w to determine mixing between water masses assumes that no source and sink terms exist, and so is not valid in surface waters, where precipitation, evaporation, run-off, melting and freezing are significant terms in the freshwater budget, except where run-off is very important and can be regarded as a separate water mass of zero salinity.

In contrast, reconstructions of palaeo-temperature and palaeo-salinity using δ_w as a conservative property assume that mixing between water masses (marine advection) is unimportant, and that the $S : \delta_w$ ratio of seawater is due only to the precipitation–evaporation cycle. This is valid only when: (1) surface waters are of unchanging origin; (2) the study area is remote from significant riverine or glacial input; and (3) in the absence of permanent or seasonal sea ice. In addition, most reconstructions assume that no changes in these conditions occurred through time, i.e. that the $S : \delta_w$ ratio over a particular region is virtually constant through time. It is thus assumed that there is no variability in the cycle of evaporation–precipitation–re-evaporation that today causes regional variation in $S : \delta_w$ ratios (Epstein and Mayeda, 1953; Dansgaard, 1964; Craig and Gordon, 1965).

Below, a simple example is presented to evaluate whether or not, and to what extent, δ_w behaves as a conservative property in the Mediterranean on geological timescales. The example is based on hypothetical changes in run-off and Black Sea input into the basin in the period 7/8k BP. The conservativeness of δ_w is assessed by comparison of the amplitude of its variations with those in salinity, a truly conservative property.

5.4.1. δ_w and S variability in the period 7/8k BP

As mentioned previously, the Mediterranean was strongly influenced by riverine input in the period 7/8k BP. Moreover, major sources of run-off were found both in the northern and in the southern parts of the basin, so that the concept of run-off as a single separate water mass of zero salinity cannot readily be used to evaluate mixing rates. Instead, run-off comprises a multitude of separate water masses of zero salinity, each with their own isotopic signatures. If all fluxes and their isotopic compositions were known, however, run-off might again be considered as a single separate water mass with an isotopic composition, δ_w^R , equal to the weighted average of all components. Also, it needs consideration that a reduced water deficit would have driven reduced Atlantic inflow, so that the marine advection term would have changed. Such changes are potentially problematic to the usual palaeoceanographic concept of conservative behaviour of δ_w . The various influences are best assessed using a simple example.

Treating total run-off as a single water mass that mixes with Atlantic inflow, the isotopic composition of Mediterranean waters *before* influences of evaporation and precipitation is given by:

$$\delta_w^{\text{Med}} = \frac{(A\delta_w^A) + (R\delta_w^R) + (B\delta_w^B)}{A + R + B} \quad (1)$$

where A is the volume of Atlantic inflow, R the total volume of run-off, B the volume of net freshwater input from the Black Sea, δ_w^A the isotopic composition of Atlantic inflow, δ_w^B the isotopic composition of net freshwater input via the Black Sea, and δ_w^R the weighted average isotopic composition of run-off. Today, A is about $23 \times 10^{12} \text{ m}^3 \text{ yr}^{-1}$ (Bryden et al., 1994); B is of order $0.1 \times 10^{12} \text{ m}^3 \text{ yr}^{-1}$ (Tolmazin, 1985), and R is of order $0.5 \times 10^{12} \text{ m}^3 \text{ yr}^{-1}$ (Garrett et al., 1993). The total water deficit (excess of

evaporation over all freshwater input; X) amounts to $1.3 \times 10^{12} \text{ m}^3 \text{ yr}^{-1}$ (Bryden et al., 1994).

Eq. 1 is dominated by the marine advection term (A), which would need to decrease considerably before the other parameters become significant. Such a decrease in A would result from a reduction in the Mediterranean water deficit. The two parameters are non-linearly related with $X/X^p \approx (A/A^p)^3$, where p stands for present-day value. Previously, a quadratic relationship was proposed (Rohling and Bryden, 1994), but recent hydraulic control models suggest that a cubed relationship is more realistic (Matthiesen and Haines, pers commun., Edinburgh, September 1997). In either case, any increase of run-off — be it directly into the Mediterranean or via the Black Sea — reduces A and so emphasises the relative influence of run-off on the value of δ_w in the Mediterranean, which amplifies δ_w depletions (positive ‘feed-back’).

The marine advection term (A) is so dominant in Eq. 1 that its relatively minor variability, as observed in contemporary inter-annual oceanographic time series, would influence salinity (S) and δ_w in more or less the same way, in spite of the fact that $\delta_w^R \neq \delta_w^B \neq 0\text{‰}$. This underlies the basic (quasi-)conservative behaviour of δ_w in the present-day Mediterranean (Rohling and Bigg, 1998). However, much greater and longer-term variations in A have been inferred for the recent geological past (e.g. Béthoux, 1984; Rohling, 1991, 1994), casting doubts on the long-term (quasi-)conservative behaviour of δ_w (Rohling and Bigg, 1998). Considering a doubling of R and B , using constant hypothetical values $\delta_w^A = 1\text{‰}$, $\delta_w^R = -5\text{‰}$, and $\delta_w^B = -9\text{‰}$ (Swart, 1991), while keeping the evaporation–precipitation cycle equal to the present, Eq. 1 indicates that the ‘feedback’ process (reduction of A with decreasing X) increases the amplitude of δ_w change by 130%, compared to 90% for the S change. These percentages are simply derived in comparison with the changes in both parameters in the absence of the ‘feedback’ (A does not change as a function of X).

We again emphasise that Eq. 1 does not incorporate influences of the evaporation–precipitation cycle. If the evaporation–precipitation cycle is assumed to have been constant through time, its influences would virtually cancel out when comparing past with present. If, in contrast, changes did oc-

cur in the evaporation–precipitation cycle, then X would be reduced further, in turn reducing A and so intensifying the ‘feedback’ mechanism.

The above shows that δ_w cannot be considered as a (quasi-)conservative property on geological time scales. There might be some scope for constraining and calibrating for the degree to which δ_w changes overestimate S changes, provided that changes in the isotopic compositions of the freshwater input terms (δ_w^B and δ_w^R) may be excluded. The literature allows evaluation of this condition. Today, δ_w^B is about -9% (Swart, 1991), but the freshwater that was being expelled from the Black Sea at 7/8k BP (Lane-Serff et al., 1997) originated (partly) from glacial meltwater and consequently may have been characterised by isotopic depletions up to those observed today in Siberia (around -15% ; Rozanski et al., 1993). The isotopic composition of palaeo-Nile waters was strongly depleted relative to the present -2% , with lacustrine carbonates suggesting a range of values reaching -10% (McKenzie, 1993) and NW African palaeo-waters suggesting a range from -8 to -13% (overview in Rozanski, 1985). Analyses on snail shells from the Negev desert suggest that local precipitation was about 2% more depleted than at present (Goodfriend, 1991). Although further quantification is needed, these arguments demonstrate that δ_w^R and δ_w^B substantially varied during the recent geological past, with likely increased depletions at 7/8k BP relative to the present. Such compositional variations in the source terms determine temporally variable non-conservative behaviour of δ_w , which causes the difference in amplitude between changes in the Mediterranean δ_w and S gradients to be even larger than discussed above.

We infer that our conclusions of water deficit reduction for 7/8k BP in the previous section were based on a parameter that overestimates the actual change, with the rate of overestimation roughly proportional to the rate of depletion in the weighted average of δ_w^R and δ_w^B relative to the present. With the weighted average of δ_w^R and δ_w^B twice as depleted as today — which may be slightly harsh but not entirely unrealistic where the Black Sea and Nile River are concerned — the amplitude of change in the Mediterranean δ_w gradient overestimates the change in S by a factor 2 to 3. The discussed change in the 7/8k BP δ_w gradient to roughly 50% of its modern

value would, in that case, correspond to a change in the S gradient to about 75% of the modern value. With $\Delta S = X^{2/3}$, this would suggest a reduction of the excess evaporation over all freshwater input (X) to roughly 65% of its modern value, instead to 35% as determined previously on the basis of assumed conservative behaviour for δ_w .

These simple calculations indicate that, to optimise the use of oxygen isotopic records from the Mediterranean, the first priority should be to determine palaeo-flux rates and — especially — palaeo-isotopic compositions of the major sources of freshwater input into the basin. In the absence of such information, the use of δ_w as a proxy for conservative properties will result in uncontrollable factor two to three times overestimations of salinity changes. Such an error severely influences reconstructions of the water deficit and palaeo-hydrography.

6. Conclusions

A robust mean glacial W–E δ_w gradient is determined of 1.5 or 1.9‰ (eastward increase), compared to present-day values of 0.4 or 0.8‰, respectively. The glacial gradient indicates that the Mediterranean acted as a concentration basin, as it does today, although there appear to have been strong relative differences in evaporation rates. The difference between the glacial and modern W–E δ_w gradients is almost entirely due to a 1‰ higher glacial mean δ_w value in the Levantine Sea. Most of this resulted from enhanced concentration effects related to sea level lowering. The remainder probably resulted from a combination of increased evaporation rates and somewhat cooler than anticipated surface waters in the glacial Levantine Sea.

The 7/8k BP δ_w gradient in the Mediterranean shows an eastward increase amounting to roughly half the magnitude of the present-day gradient, but of similar sign. This suggests that the Mediterranean continued to act as a concentration basin, albeit with lower intensity than at present. Values in the Levantine basin appear to have undergone up to 0.3‰ more depletion than those in the rest of the eastern Mediterranean. This amplification is interpreted: (1) as an expression of strong influence of Nile discharge in the shallow, late summer, mixed-layer, which would support previous hypotheses of summer monsoon

driven maxima of the Nile discharge around 7/8k BP, although the present study identifies no significant geographic trends in the depletion within the Levantine basin; and/or (2) as a result of stronger isotopic depletion in the Nile discharge at times of sapropel formation; and/or (3) in terms of a possible error of order 1.5°C in the assumption that the temperature distribution over the eastern Mediterranean was similar to the present, when considering effects on δ_w to δ_{fc} fractionation; and/or (4) in terms of a slightly decreased rate of evaporation over the Levantine basin.

Simple mixing arguments demonstrate that enhanced freshwater input into the basin would cause stronger decreases in δ_w than in salinity. Use of isotopic differences between periods of high freshwater input and the present will, therefore, result in significant overestimates of salinity differences. Even when assuming that the isotopic composition of run-off was constant through time, the isotopic changes appear to be a factor 1.5 higher than the salinity changes. If run-off was isotopically more depleted, which is argued to have been likely for the period between 7 and 8 ka BP, this difference rises to well over a factor 2. In other words, the slope of the $S : \delta_w$ mixing line rapidly becomes more than twice as steep as the present, which has major implications for further palaeoceanographic interpretations.

Acknowledgements

We thank G. Bigg, K. Haines, A. Kemp, S. Matthiesen, P. Myers, M. Paterne, M. Rossignol-Strick, and N. Wells for discussions and comments, H. Buckley, R. Thunell and D. Williams for contributing relevant unpublished data to our (EC Mast-3 CLIVAMP) LGM–Present Mediterranean palaeo-database, and W. Berger and C. Pierre for their constructive reviews. This study is supported by EC Mast-3 programme Climatic Variability of the Mediterranean Palaeocirculation (CLIVAMP; MAS3-CT95-0043) and Leverhulme Trust project ‘Oxygen isotopes: disentangling a record of oceanic and atmospheric variability’ (F/204/Q). It contributes to UNESCO–IUGS program Climates in the Past (CLIP).

References

- Aksu, A.E., Yasar, D., Mudie, P.J., Gillespie, H., 1995. Late glacial–Holocene paleoclimatic and paleoceanographic evolution of the Aegean Sea: micropaleontological and stable isotopic evidence. *Mar. Micropaleontol.* 25, 1–28.
- Beer, T., 1990. Applied Environmetrics Meteorological Tables. Applied Environmetrics, Victoria, Australia, 56 pp.
- Béthoux, J.P., 1984. Paléo-hydrologie de la Méditerranée au cours des derniers 20,000 ans. *Oceanol. Acta* 7, 43–48.
- Béthoux, J.P., Gentili, B., 1996. The Mediterranean Sea, coastal and deep-sea signatures of climatic and environmental changes. *J. Mar. Syst.* 7, 383–394.
- Bigg, G.R., 1995. Aridity of the Mediterranean Sea at the last glacial maximum: a reinterpretation of the $\delta^{18}\text{O}$ record. *Paleoceanography* 10, 283–290.
- Blanchon, P., Shaw, J., 1995. Reef drowning during the last deglaciation: Evidence for catastrophic sea-level rise and ice-sheet collapse. *Geology* 23, 4–8.
- Bryden, H.L., Kinder, T.H., 1991. Steady two-layer exchange through the Strait of Gibraltar. *Deep-Sea Res.* 38 (Suppl. 1), s445–s463.
- Bryden, H.L., Candela, J., Kinder, T.H., 1994. Exchange through the Strait of Gibraltar. *Prog. Oceanogr.* 33, 201–248.
- Buckley, H.A., Johnson, L.R., 1988. Late Pleistocene to Recent sediment deposition in the central and western Mediterranean. *Deep-Sea Res.* 35, 749–766.
- Buckley, H.A., Johnson, L.R., Shackleton, N.J., Blow, R.A., 1982. Late Glacial to Recent sediment cores from the eastern Mediterranean. *Deep-Sea Res.* 29, 739–766.
- Cheddadi, R., Rossignol-Strick, M., Fontugne, M., 1991. Eastern Mediterranean palaeoclimates from 26 to 5 ka BP documented by pollen and isotopic analysis of a core in the anoxic Bannock Basin. *Mar. Geol.* 100, 53–66.
- Craig, H., Gordon, L.I., 1965. Isotopic oceanography: deuterium and oxygen 18 variations in the ocean and the marine atmosphere. In: Tongiorgi, E. (Ed.), *Stable Isotopes in Oceanographic Studies and Paleotemperatures*. Consiglio Nazionale di Recherche, Spoleto, pp. 9–130.
- Dansgaard, W., 1964. Stable isotopes in precipitation. *Tellus* 16, 436–468.
- Davis, J.C., 1986. *Statistics and Data Analysis in Geology* (2nd ed.). Wiley, New York, 646 pp.
- Epstein, S., Mayeda, T., 1953. Variation of $\delta^{18}\text{O}$ content of waters from natural sources. *Geochim. Cosmochim. Acta* 4, 213–224.
- Fairbanks, R.G., 1982. The origin of continental shelf and slope water in the New York Bight and Gulf of Maine: evidence from $\text{H}_2^{18}\text{O}/\text{H}_2^{16}\text{O}$ ratio measurements. *J. Geophys. Res.* 87, 5796–5808.
- Fairbanks, R.G., 1989. A 17,000 year glacio-eustatic sea level record: Influence of glacial melting rates on the Younger Dryas event and deep-ocean circulation. *Nature* 342, 637–642.
- Fairbanks, R.G., 1990. The age and origin of the ‘Younger Dryas Climate Event’ in Greenland Ice Cores. *Paleoceanography* 5, 937–948.
- Fontugne, M.R., Calvert, S.E., 1992. Late Pleistocene variability

- of the organic carbon isotopic composition of organic matter in the eastern Mediterranean: monitor of changes in organic carbon sources and atmospheric CO₂ concentrations. *Paleoceanography* 7, 1–20.
- Fontugne, M.R., Paterne, M., Calvert, S.E., Murat, A., Guichard, F., Arnold, M., 1989. Adriatic deep water formation during the Holocene: implication for the reoxygenation of the deep eastern Mediterranean Sea. *Paleoceanography* 4, 199–206.
- Fontugne, M., Arnold, M., Labeyrie, L., Paterne, M., Calvert, S., Duplessy, J.-C., 1994. Paleoenvironment, sapropel chronology, and Nile river discharge during the last 20,000 years as indicated by deep-sea sediment records in the eastern Mediterranean. *Radiocarbon* 34, 75–88.
- Frew, R.D., Heywood, K.J., Dennis, P.F., 1995. Oxygen isotope study of water masses in the Princess Elizabeth Trough, Antarctica. *Mar. Chem.* 49, 141–153.
- Garrett, C., Outerbridge, R., Thompson, K., 1993. Interannual variability in Mediterranean heat budget and buoyancy fluxes. *J. Climatol.* 6, 900–910.
- Goodfriend, G.A., 1991. Holocene trends in ¹⁸O in snail shells from the Negev desert and their implications for changes in rainfall source areas. *Quat. Res.* 35, 417–426.
- Hemleben, C., Meischner, D., Zahn, R., Almogi-Labin, A., Erlenkeuser, H., Hiller, B., 1996. Three hundred eighty thousand year long stable isotope and faunal records from the Red Sea: influence of global sea level change on hydrography. *Paleoceanography* 11, 147–156.
- Jenkins, J.A., Williams, D.F., 1984. Nile water as a cause of eastern Mediterranean sapropel formation: evidence for and against. *Mar. Micropaleontol.* 9, 521–534.
- Jorissen, F.J., Asioli, A., Borsetti, A.M., Capotondi, L., De Visser, J.P., Hilgen, F.J., Rohling, E.J., Van der Borg, K., Vergnaud-Grazzini, C., Zachariasse, W.J., 1993. Late Quaternary central Mediterranean biochronology. *Mar. Micropaleontol.* 21, 169–189.
- Kallel, N., Paterne, M., Duplessy, J.-C., Vergnaud-Grazzini, C., Pujol, C., Labeyrie, L., Arnold, M., Fontugne, M., Pierre, C., 1997. Enhanced rainfall in the Mediterranean region during the last sapropel event. *Oceanol. Acta*, in press.
- Kipphut, G.W., 1990. Glacial meltwater input to the Alaska coastal current: evidence from oxygen isotope measurements. *J. Geophys. Res.* 95, 5177–5181.
- Labeyrie, L.D., Duplessy, J.-C., Blanc, P.L., 1987. Variations in the mode of formation and temperature of oceanic deep waters over the past 125,000 years. *Nature* 327, 477–482.
- Labeyrie, L., Labracherie, M., Gorfti, N., Pichon, J.J., Vautravers, M., Arnold, M., Duplessy, J.-C., Paterne, M., Michel, E., Duprat, J., Caralp, M., Turon, J.-L., 1996. Hydrographic changes of the Southern ocean (southeast Indian sector) over the last 230 kyr. *Paleoceanography* 11, 57–76.
- Lane-Serff, G.F., Rohling, E.J., Bryden, H.L., Charnock, H., 1997. Post-glacial connection of the Black Sea to the Mediterranean and its relation to the timing of sapropel formation. *Paleoceanography* ('Currents') 12, 169–174.
- Luz, B., 1979. Palaeo-oceanography of the postglacial Mediterranean. *Nature* 278, 847–848.
- Maslin, M.A., Shackleton, N.J., Pflaumann, U., 1995. Surface water temperature, salinity, and density changes in the north-east Atlantic during the last 45,000 years: Heinrich events, deep water formation, and climatic rebounds. *Paleoceanography* 10, 527–544.
- McKenzie, J.A., 1993. Pluvial conditions in the eastern Sahara following the penultimate deglaciation: implications for changes in atmospheric circulation patterns with global warming. *Palaeogeogr., Palaeoclimatol., Palaeoecol.* 103, 95–105.
- Mix, A., Ruddiman, W., 1984. Oxygen isotope analyses and Pleistocene ice volumes. *Quat. Res.* 21, 1–20.
- Nof, D., 1979. On man-induced variations in the circulation of the Mediterranean Sea. *Tellus* 31, 558–564.
- O'Neil, J., Clayton, R., Mayeda, T., 1969. Oxygen isotope fractionation in divalent metal carbonates. *J. Chem. Phys.* 51, 5547–5558.
- Paterne, M., Guichard, F., Labeyrie, L., Gillot, P.Y., Duplessy, J.-C., 1986. Tyrrhenian Sea tephrochronology of the oxygen isotope record for the past 60,000 years. *Mar. Geol.* 72, 259–285.
- Pierre, C., 1999. The oxygen and carbon isotope distribution in the Mediterranean water masses. *Mar. Geol.* 153, 41–55.
- Pierre, C., Vergnaud-Grazzini, C., Thouron, D., Saliège, J.-F., 1986. Compositions isotopiques de l'oxygène et du carbone des masses d'eau en Méditerranée. *Mem. Soc. Geol. Ital.* 36, 165–174.
- Pujol, C., Vergnaud-Grazzini, C., 1989. Palaeoceanography of the last deglaciation in the Alboran Sea (western Mediterranean). Stable isotopes and planktonic foraminiferal records. *Mar. Micropaleontol.* 15, 153–179.
- Pujol, C., Vergnaud-Grazzini, C., 1995. Distribution patterns of live planktic foraminifera as related to regional hydrography and productive systems of the Mediterranean Sea. *Mar. Micropaleontol.* 25, 187–217.
- Rohling, E.J., 1991. A simple two-layered model for shoaling of the eastern Mediterranean pycnocline due to glacio-eustatic sea-level lowering. *Paleoceanography* 6, 537–541.
- Rohling, E.J., 1994. Review and new aspects concerning the formation of eastern Mediterranean sapropels. *Mar. Geol.* 122, 1–28.
- Rohling, E.J., Bigg, G.R., 1998. Paleosalinity and $\delta^{18}\text{O}$: a critical assessment. *J. Geophys. Res. (Oceans)* 103, 1307–1318.
- Rohling, E.J., Bryden, H.L., 1992. Man-induced salinity and temperature increases in western Mediterranean deep water. *J. Geophys. Res.* 97, 11191–11198.
- Rohling, E.J., Bryden, H.L., 1994. A method for estimating past changes in the eastern Mediterranean freshwater budget, using reconstructions of sea level and hydrography. *Proc. K. Ned. Akad. Wetensch.* 97, 201–217.
- Rohling, E.J., Hilgen, F.J., 1991. The eastern Mediterranean climate at times of sapropel formation: a review. *Geol. Mijnbouw* 70, 253–264.
- Rohling, E.J., Jorissen, F.J., Vergnaud-Grazzini, C., Zachariasse, W.J., 1993. Northern Levantine and Adriatic Quaternary planktic foraminifera; reconstruction of paleoenvironmental gradients. *Mar. Micropaleontol.* 21, 191–218.
- Rohling, E.J., Jorissen, F.J., De Stigter, H.C., 1997. 200 Year

- interruption of Holocene sapropel formation in the Adriatic Sea. *J. Micropalaeontol.*, in press.
- Rossignol-Strick, M., 1987. Rainy periods and bottom water stagnation initiating brine accumulation and metal concentrations, 1. The Late Quaternary. *Paleoceanography* 2, 333–360.
- Rossignol-Strick, M., Nesteroff, V., Olive, P., Vergnaud-Grazzini, C., 1982. After the deluge; Mediterranean stagnation and sapropel formation. *Nature* 295, 105–110.
- Rozanski, K., 1985. Deuterium and oxygen-18 in European groundwaters — links to atmospheric circulation in the past. *Chem. Geol. (Isot. Geosci. Sect.)* 52, 349–363.
- Rozanski, K., Araguás-Araguás, L., Gonfiantini, R., 1993. Isotopic patterns in modern global precipitation. In: Swart, P.K., Lohmann, K.C., McKenzie, J., Savin, S. (Eds.), *Climate Change in Continental Isotopic Records*. AGU Geophys. Monogr. 78, 1–36.
- Shackleton, N.J., 1987. Oxygen isotopes, ice volume and sea-level. *Quat. Sci. Rev.* 6, 183–190.
- Shaw, H.F., Evans, G., 1984. The nature, distribution and origin of a sapropelic layer in sediments of the Cilicia Basin, northeastern Mediterranean. *Mar. Geol.* 61, 1–12.
- Sikes, E.L., Keigwin, L.D., 1994. Equatorial Atlantic sea surface temperature for the last 30 kyr: A comparison of U^{k}_{37} , $\delta^{18}O$ and foraminiferal assemblage temperature estimates. *Paleoceanography* 9, 31–45.
- Squires, G.L., 1988. *Practical Physics* (3rd ed. with rev.). Cambridge University Press, Cambridge, 213 pp.
- Swart, P.K., 1991. The oxygen and hydrogen isotopic of the Black Sea. *Deep-Sea Res.* 38 (Suppl. 2), s761–s772.
- Tang, C.M., Stott, L.D., 1993. Seasonal salinity changes during Mediterranean sapropel deposition 9000 years B.P.: evidence from isotopic analyses of individual planktonic foraminifera. *Paleoceanography* 8, 473–493.
- Thunell, R.C., Williams, D.F., 1989. Glacial–Holocene salinity changes in the Mediterranean Sea: hydrographic and depositional effects. *Nature* 338, 493–496.
- Tolmazin, D., 1985. Changing coastal oceanography of the Black Sea, I. Northwestern Shelf. *Prog. Oceanogr.* 15, 217–276.
- Troelstra, S.R., Ganssen, G.M., Van der Borg, K., De Jong, A.F.M., 1991. A Late Quaternary stratigraphic framework for eastern Mediterranean sapropel S₁ based on AMS ^{14}C dates and stable isotopes. *Radiocarbon* 33, 15–21.
- Vergnaud-Grazzini, C., Ryan, W.B.F., Cita, M.B., 1977. Stable isotope fractionation, climatic change and episodic stagnation in the eastern Mediterranean during the late Quaternary. *Mar. Micropaleontol.* 2, 353–370.
- Vergnaud-Grazzini, C., Devaux, M., Znaidi, J., 1986a. Stable isotope ‘anomalies’ in Mediterranean Pleistocene records. *Mar. Micropaleontol.* 10, 35–69.
- Vergnaud-Grazzini, C., Glaçon, G., Pierre, C., Pujol, C., Urrutiaguer, M.J., 1986b. Foraminifères planctoniques de Méditerranée en fin d’été. Relations avec les structures hydrologiques. *Mem. Soc. Geol. Ital.* 36, 175–188.
- Vergnaud-Grazzini, C., Borsetti, A.M., Cati, F., Colantoni, P., d’Onofrio, S., Saliège, J.F., Sartori, R., Tampieri, R., 1988. Palaeoceanographic record of the last deglaciation in the Strait of Sicily. *Mar. Micropaleontol.* 13, 1–21.
- Wahby, S.D., Bishara, N.F., 1981. The effect of the River Nile on Mediterranean water, before and after the construction of the High Dam at Aswan. In: Martin, J.-W., Burton, J.D., Eisma, D. (Eds.), *River Input to Ocean Systems*. Proc. SCOR/ACMRR/ECOR/IAHS/UNESCO/CMG/IABO/IAPSO Review and Workshop at FAO Headquarters, 26–30 March 1979, Rome. UNEP & UNESCO (Switzerland), pp. 311–318.
- Weiss, R.F., Östlund, H.G., Craig, H., 1979. Geochemical studies of the Weddell Sea. *Deep-Sea Res.* 26A, 1093–1120.
- Wells, N.C., 1995. Surface heat fluxes in the western equatorial Pacific Ocean. *Ann. Geophys.* 13, 1047–1053.
- Wells, N.C., King-Hele, S., 1990. Parameterization of tropical ocean heat flux. *Q. J. R. Meteorol. Soc.* 116, 1213–1224.
- Zachariasse, W.J., Jorissen, F.J., Perissoratis, C., Rohling, E.J., Tsapralis, V., 1997. Late Quaternary foraminiferal changes and the nature of sapropel S₁ in Skopelos Basin. *Proc. 5th Hellenic Symp. Oceanography and Fisheries, Kavalla*, 15–18 April, 1997, Vol. 1, pp. 391–394.